CAMES, **27**(2–3): 185–204, 2020, doi: 10.24423/cames.281

Michell Structures within L-Shaped Domains

Karol BOŁBOTOWSKI[1,2)*], Tomasz LEWIŃSKI[1)], Tomasz SOKÓŁ[1)]

[1)] *Faculty of Civil Engineering*
Warsaw University of Technology
al. Armii Ludowej 16, 00-637 Warsaw, Poland
*Corresponding Author e-mail: k.bolbotowski@il.pw.edu.pl

[2)] *College of Inter-Faculty Individual Studies in Mathematics and Natural Sciences*
University of Warsaw
Stefana Banacha 2C, 02-097 Warsaw, Poland

By recalling the main mathematical results concerning the theory of Michell structures, the present paper puts forward an interpretation of the selected numerical methods for constructing their approximants, that is, trusses with a large number of nodes. The efficiency of one of these methods: the ground structure method in its adaptive version is shown in the context of the L-shaped design domain problem. A large family of highly accurate truss approximants corresponding to the point loads acting at selected vertices is constructed and discussed.

Keywords: Michell structures, structural optimization, trusses.

1. Introduction

The planar Michell structures are fully stressed plane frames of the least volume, designed in a given admissible domain Ω, transmitting a given static load F to a given supporting contour, see Hemp [5] and Lewiński *et al.* [8]. Optimization leads to the stress distribution being uniform across the bars thicknesses; the stress σ is subject to the lower and upper bounds: $-\sigma_C \leq \sigma \leq \sigma_T$, where σ_C, σ_T represent the permissible stresses in compression and tension. The equilibrium equations are referred to the undeformed configuration. Hence, the buckling problems lie outside the scope of this theory.

The present paper focuses on Michell layouts within the L-shaped domains, thus extending the previous studies by Lewiński and Rozvany [6] and Lewiński *et al.* [7]. The former paper included an error, corrected in the latter paper. The hitherto known solutions referring to the L-shaped domain are gathered in Sec. 4.15.1.1 in Lewiński *et al.* [8].

The aim of the present paper is to put forward two families of Michell solutions within the L-shaped domain, corresponding to the point loads at the vertices E or F, see Figs 1a and 1b. Each of the two families is parameterized by the angle α of inclination of the force P applied at two different points, respectively. The exact solutions are known only for very specific cases: if $\alpha = 0$ or $\alpha = \pi$, for both positions of the point load: at E or F, the solution becomes trivial (one bar) if the point load is at F and $\alpha = \pi/4$. This study extends this modest family of known exact solutions (corresponding to the points of application of the force at E or F) to the case of the load applied at vertex E, for $0 \leq \alpha \leq \pi/4$. Other cases would raise essential difficulties while constructing the exact solutions. Nowadays, however, the exact solutions are not so important as in the past, since the *ground structure method* developed for Michell problems by Gilbert and Tyas [4] has paved the way towards highly accurate numerical solutions. Therefore, this paper mainly aims at constructing the approximate solutions to encompass all possible values of the angle α thus showing the whole structural morphology driven by the rotating force. The solutions are constructed using the *ground structure method* in the version proposed by Sokół [9, 10] and Bołbotowski and Sokół [1]. The method is presented in detail in Sec. 3 and made suitable for the problems discussed.

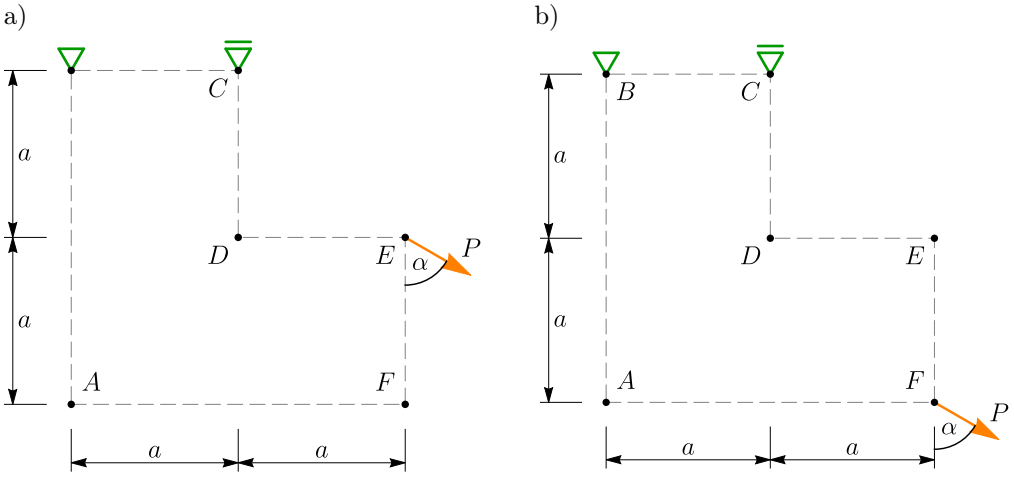

FIG. 1. The problem setting: a) the force applied at the right upper vertex E; b) the force applied at the right lower vertex F; the dashed line denotes the boundary of the design domain.

The computations are performed for the case of $\sigma_C = \sigma_T = \sigma_0$. Nevertheless, the constructed results extend towards the general case of $\sigma_C \neq \sigma_T$ according to Maxwell's method, see Lewiński *et al.* [8], Sec. 2.2.3. The latter method applies if Michell structures are externally statically determinate, which is the case

here: the reactions can be directly computed by solving the system of global equilibrium. This is discussed in Final Remarks.

2. Theoretical background

The theory of Michell structures is best developed for scenario with equal permissible stresses in tension and compression, i.e., for $\sigma_C = \sigma_T = \sigma_0$. In this case, Michell structures can be alternatively viewed as the least compliant elastic frames of a given volume. Under the condition $\sigma_C = \sigma_T$, both the problems mentioned: the problem of the volume minimization and the problem of the compliance minimization reduce to the two mutually dual problems. In the simpler scenario, when the kinematical supports are absent with the load F being self-equilibrated, this duality pair reads as follows, see Bouchitté *et al.* [3]:

$$Z_1 = \sup\left\{\int \langle F, u\rangle \,\middle|\, \rho\left(\varepsilon\left(u\right)\right) \leq 1 \quad \text{in} \quad \Omega, \;\; u \in C^1\left(\overline{\Omega};\, \mathbb{R}^2\right)\right\}, \tag{1}$$

$$Z_2 = \min\left\{\int \rho^0\left(\sigma\right) \,\middle|\, \sigma \in \mathcal{M}\left(\overline{\Omega}; \mathcal{S}^{2\times 2}\right), \;\; \operatorname{div}\sigma + F = 0\right\}. \tag{2}$$

Here Ω is a bounded and connected open set of $\mathbb{R}^2$, with Lipschitz boundary, the load is represented by a vector-valued Radon measure $F \in \mathcal{M}\left(\overline{\Omega};\, \mathbb{R}^2\right)$ that, for example, encompasses the class of point loads both in the interior of Ω and on the boundary $\partial\Omega$. The symbol $\mathcal{M}\left(\overline{\Omega};\, \mathcal{S}^{2\times 2}\right)$ denotes the space of Radon measures supported in $\overline{\Omega}$ with values in the space of symmetric tensors $\mathcal{S}^{2\times 2}$ and $\varepsilon(u)$ is the symmetric part of the gradient of a vector-valued function u. The equilibrium equation $\operatorname{div}\sigma + F = 0$ is valid when intended in the sense of distributions on the whole $\mathbb{R}^2$. For the integral $\displaystyle\int \rho^0(\sigma)$ to be well-defined, the function ρ must be 1-homogeneous, convex and an estimate

$$k\left|\varepsilon\right| \leq \rho\left(\varepsilon\right) \leq K\left|\varepsilon\right| \quad \forall \varepsilon \in \mathcal{S}^{2\times 2}, \tag{3}$$

must hold for certain positive numbers k, K. The pair of problems (1) and (2) becomes precisely Michell problem whenever (just for the case of $\sigma_C = \sigma_T$) the function ρ is the spectral norm while ρ^0 is its polar; here:

$$\rho\left(\varepsilon\right) = \max_{1\leq i\leq 2}\left|\lambda_i\left(\varepsilon\right)\right|, \qquad \rho^0\left(\sigma\right) = \sum_{i=1}^{2}\left|\lambda_i(\sigma)\right|, \tag{4}$$

where $\lambda_i\left(\cdot\right)$ is the i-th eigenvalue of the argument (matrix). According to Bouchitté and Fragalà [2] the pair of problems (1) and (2) is well-posed, more

precisely the problem (2) attains a solution $\widehat{\sigma} \in \mathcal{M}\left(\overline{\Omega}; \mathcal{S}^{2\times 2}\right)$ while the problem (1) requires relaxing the differentiability condition, see (5) below. Moreover, $Z_1 = Z_2 = Z$, i.e., the duality gap vanishes.

The solution to Michell problem is a pair of fields: $\widehat{\sigma}$ being the minimizer of (2) and $\widehat{u}$ – the maximizer of a relaxed version of (1). The optimal structure occupies the subdomain $\mathrm{spt}(\widehat{\sigma}) \subset \overline{\Omega}$ and the other part of the design domain is not used. In the case of point loads, it is typical that the boundary of this subdomain is charged by the measure $\widehat{\sigma}$, i.e., the optimal body concentrates on the part of this boundary in the form of straight or curved bars. This boundary and the trajectories of the principal stresses of $\widehat{\sigma}$ are the main unknowns.

We put forward a reformulation of the displacement-based problem (1):

$$Z = \max\left\{ \int \langle F, u\rangle \,|\, u \in \mathcal{U}_1(\Omega) \right\}, \tag{5}$$

where $\mathcal{U}_1(\Omega)$ is a subset of the space of continuous vector-valued functions $u \in C\left(\overline{\Omega}; \mathbb{R}^2\right)$ that satisfy a two-point condition

$$-|x-y| \le \left\langle u(x) - u(y), \frac{x-y}{|x-y|} \right\rangle \le |x-y| \qquad \forall [x,y] \subset \overline{\Omega}, \quad x \neq y, \tag{6}$$

where $\langle \cdot, \cdot \rangle$ denotes the scalar product of vectors, while $[x, y]$ is a straight segment connecting points x and y. For convex design domains Ω, the equivalence between the problems (1) and (2) was proved in Bouchitté *et al.* [3], see Lemma 2.1 therein, where condition (6) is naturally checked for all the pairs of distinct points $x, y \in \overline{\Omega}$. The proof of this equivalence, however, can be easily extended to arbitrary domains Ω once the pairs x, y testing the inequalities in (6) are restricted to those for which $[x, y]$ is contained in $\overline{\Omega}$. It should be stressed that, in contrast to the problem (1) that requires differentiability of u, the solution of the problem (5) always exists (we assume that load F is self-equilibrated and that the boundary $\partial\Omega$ is at least Lipschitz regular).

3. The discrete formulation of Michell problem

3.1. A word of motivation

Numerous exact solutions to Michell problem available in the literature imply that the solutions to problems (1) and (2) can be approximated by sequences of truss-type solutions to the considered optimization problem corresponding to the given load F and given design domain. The approximative sequences are usually constructed fixing regular grids of points of coordinates (mb, nb), with a selected size of a cell of the grid $b > 0$ and with n, m being integer numbers ranging in such a way that $(mb, nb) \in \overline{\Omega}$; such grids shall be denoted by $X \subset \overline{\Omega}$ being a finite set.

The load F will be assumed to consist of point forces applied at points of X only. In the optimization process, we find connections between the nodes of the grids, being nodes of possible trusses forming within the design domain. The position of truss nodes fixes the lengths of the truss members. The process of optimization leads to the stress state in the truss being distributed uniformly, attaining the bounds $\pm\sigma_0$. The essential feature of the theory of Michell structures is that their exact solutions are available for a wide variety of data; now we know that they can be approximated highly accurately by the trusses of a finite number of members.

Historically Michell problem (both the formulations (1) and (2) appeared for the first time in Strang and Kohn [11]) was proposed as a relaxation of the classical truss optimization problem. Therefore, numerical treatment of the problem via approximation by finite, yet very dense trusses is natural and was first applied with great efficiency in Gilbert and Tyas [4]. Nevertheless, in this short subsection, we propose another perspective that sheds light on a direct link between the truss problem and Michell problem (1) and (2), while, to that aim, we shall employ formulation (5).

For a chosen finite grid X let (with a slight abuse of notation) $\mathcal{U}_1(X)$ stand for the set of continuous functions $u \in C(\overline{\Omega}; \mathbb{R}^2)$ for which the two-point condition (6) is tested only for distinct pairs of points $x, y \in X$, which additionally, in case of a non-convex domain Ω, satisfy $[x, y] \subset \overline{\Omega}$. Then, since $\mathcal{U}_1(X)$ is less constrained than $\mathcal{U}_1(\Omega)$, the following estimate holds:

$$Z \leq Z_X = \max\left\{ \int \langle F, u \rangle \;\middle|\; u \in \mathcal{U}_1(X) \right\}. \tag{7}$$

Since the load F is assumed to be supported in the finite set X, in (7) clearly the virtual displacement values $u(x)$ matter only at $x \in X$ rendering this problem discrete. Readily, the term $\langle u(x) - u(y), (x-y)/|x-y| \rangle$ may be recognized as elongation of a truss bar that potentially connects the nodes $x, y \in X$. One may expect that assuming a sequence of grids X_h consisting of points $(mb_h, nb_h) \in \overline{\Omega}$ with $b_h = b_0/2^h \to 0$, monotonic convergence $Z_{X_h} \searrow Z$ should hold when h goes to infinity. We easily discover that (7) is a finite dimensional linear programming problem and thus it is natural to pass from the somewhat abstract setting in (7) to an algebraic/matrix formulation, which we shall do in the next subsection, including deriving the dual formulation for (7) being a discrete counterpart of the stress-based problem (2).

We conclude this introductory section with yet another remark: the fact that the problem (1) could be rewritten with the use of the two-point condition (6) is not a feature of the problem (1) itself, but rather an exceptional property of the spectral norm ρ displayed in (4). This distinguishes Michell problem from the other shape optimization problems known in the literature (see Bouchitté

and Fragalà [2]) and essentially justifies the discretized approach employed in this paper.

3.2. Algebraic formulation of the discrete problem

Let us consider a special family of problems of optimum design of trusses. Assume that the grid points of coordinates $(mb, nb) \in X$, m, n being integer numbers, lie within the design domain $\overline{\Omega}$. This choice depends on the position of the coordinate system's origin and the choice of the parameter $b > 0$.

A system of point loads P_j (acting in the horizontal or vertical direction depending on the index j), $j = 1, ..., N$ within $\overline{\Omega}$ and the places of fixed hinges and roller supports is given, like in Fig. 1. The aim is to find the least volume truss in the bars in which the stresses lie within the range $-\sigma_0 \leq \sigma \leq \sigma_0$. The design variables are areas of cross-sections A_k, $k = 1, ..., M$. The zero cross-sections are admitted: $A_k \geq 0$. The length of the bar of number k is L_k. A given configuration of all bars, which shall be henceforward called a *ground structure*, fixes the geometric matrix $\mathbf{B}$ of dimensions M by N; this matrix links the elongations of bars Δ_k with the displacements of nodes u_j:

$$\boldsymbol{\Delta} = \mathbf{B}\mathbf{u}, \qquad \mathbf{u} \in \mathbb{R}^N. \tag{8}$$

The axial forces in the truss members are denoted by T_k if the member force is non-negative and, by $-C_k$, otherwise. Thus $T_k \geq 0$, $C_k \geq 0$, $T_k C_k = 0$. The equations of equilibrium of the nodes can be written in the form:

$$\mathbf{B}^T(\mathbf{T} - \mathbf{C}) = \mathbf{P}. \tag{9}$$

As it has been proved by Hemp [5] the problem of the volume minimization with the condition $-\sigma_0 \leq \sigma \leq \sigma_0$ reduces to the following pair of mutually dual linear programming (LP) problems:

$$\begin{aligned} &\max \ \mathbf{P}^T\mathbf{u} \\ &\text{over} \ \ \mathbf{u} \in \mathbb{R}^N \\ &\qquad -\mathbf{L} \leq \mathbf{B}\mathbf{u} \leq \mathbf{L} \end{aligned} \tag{10}$$

and

$$\begin{aligned} &\min \ \mathbf{L}^T(\mathbf{T} + \mathbf{C}) \\ &\text{over} \ \ \mathbf{T} \in \mathbb{R}^M, \ \mathbf{C} \in \mathbb{R}^M \\ &\qquad \mathbf{B}^T(\mathbf{T} - \mathbf{C}) = \mathbf{P} \\ &\qquad \mathbf{T} \geq \mathbf{0}, \ \mathbf{C} \geq \mathbf{0}, \end{aligned} \tag{11}$$

where

$$\mathbf{L} = [L_1, ..., L_M]^T, \qquad \mathbf{T} = [T_1, .., T_M]^T, \qquad \mathbf{C} = [C_1, ..., C_M]^T,$$
$$\mathbf{P} = [P_1, ..., P_N]^T, \qquad \mathbf{u} = [u_1, ..., u_N]^T.$$

In the constraint $(10)_3$, one can recognize the two-point condition (6): indeed, the number $\Delta_k = (\mathbf{Bu})_k$ represents elongation of the k-th bar potentially connecting a certain pair of points $(x_k, y_k) \in X \times X$, while $L_k = |x_k - y_k|$ is the length of this bar. Therefore, the problem (10) is the discrete version of the displacement-based Michell problem (1), while (11) is the finite dimensional approximation of (2).

3.3. The adaptive ground structure approach

The pair of finite dimensional problems (10) and (11), even for moderately dense ground structures, becomes too large for direct treatment using either simplex or interior point methods. To overcome this obstacle, the method of selective subsets of active bars can be used instead (see Gilbert and Tyas [4], Sokół [9, 10]). The main idea of this method is to replace one large LP problem (11) by an appropriate series of significantly smaller sub-problems that are solved iteratively. In the first iteration, the initial ground structure includes only the bars connecting the neighboring nodes, see Fig. 2a. In the next iterations, longer and longer connections are considered as the candidate bars for addition into the current ground structure, see Figs 2b–d. The level of connectivity is defined by the parameter $dist = \max(dix, diy)$, where dix and diy denote the increments of nodal numbering in x and y directions, respectively. As shown in Fig. 2, the bars outside the feasible domain are removed and cannot participate in the transfer of forces. The appropriate filtering scheme of allowable connections is presented in Bołbotowski and Sokół [1] and will not be discussed in detail here.

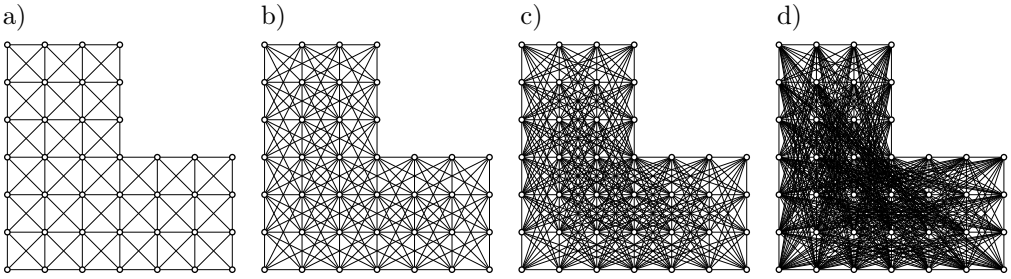

FIG. 2. Ground structures for L-shaped domain with increasing level of connectivity: a) $dist = 1$ – bars connect only the adjacent nodes, b) $dist = 2$, c) $dist = 3$, d) $dist = 6$ – fully connected ground structure with 438 potential bars.

The step by step algorithm of the adaptive ground structure method is as follows:

Initialization of data structures:

0. Prepare data for efficient handling of large-scale but regular ground structures of increasing level of connectivity:
   - for preserving a big amount of RAM and CPU, the patterns of elements are used to represent the whole family of bars with identical directional cosines (the full table of all potential elements is not necessary and was never created because it clearly could be too large),
   - the applied database is also convenient for vectorization and parallel computing.

First iteration:

1. Set $iter = 1$ and $dist = 1$.
2. Set the initial ground structure with bars connecting only the most neighboring nodes (see Fig. 2a). These bars create a stable groundwork that allows obtaining nodal displacements in the whole design domain, even in 'empty zones', where no material is needed.
3. Solve primal subproblem (11) and also obtain dual variables $\mathbf{u}^{(1)}$ of the corresponding subproblem (10).

Next iterations:

4. Increase *iter* and *dist*.
5. Select the set of active bars for a ground structure with a new level of connectivity:
   - for every k-th new potential bar, calculate its strain $\varepsilon_k = \Delta_k / L_k$ (see Eq. (8)) and if $|\varepsilon_k| \geq 1$ then activate it (add this bar to the new set of active bars),
   - if the number of added bars is too small and $dist < dist_{\max}$ then increment *dist* and repeat step 5 with a longer level of connectivity.
6. Check the stopping criterion:
   - if $dist = dist_{\max}$ and there are no new bars added in step 5, then finish. The optimum solution is found because constraints $(10)_3$ are satisfied for all potential bars and the solution cannot be further improved.
7. Solve the next primal subproblem (11) and also obtain dual variables $\mathbf{u}^{(iter)}$ of the corresponding subproblem (10).
8. Repeat from step 4.

It should be noted that usually only a small subset of new candidate bars is worth adding into subsequent ground structures, thus subproblems of the form (11) for only m active bars, where $m \ll M$, have to be solved in succeeding iterations. Moreover, using the primal-dual version of the interior point method, apart from the primal variables $\mathbf{T}$ and $\mathbf{C}$ from (11), we also obtain dual variables $\mathbf{u}$ in (10) without additional computational time. Note that constraints $(10)_3$ correspond to the well-known Michell optimality criteria, which have to be satisfied in the optimal solution. If any of these constraints are violated in a fully connected ground structure, then the solution is not optimal and can be improved by adding corresponding bars into the current, yet not to the final ground structure. This important observation was firstly noted by Gilbert and Tyas [4] and is also used in the method developed by the third author of the present paper. This observation results directly from the strong duality theorem, which indicates that for an optimal solution (if such exists), the values of the objective functions of the primal and dual forms are equal: $\max \mathbf{P}^T\ \mathbf{u} = \min \mathbf{L}^T(\mathbf{T} + \mathbf{C})$. Adding new bars into the current ground structure is equivalent to adding new constraints $(10)_3$ in the dual form, which cannot increase (it usually decreases) $\mathbf{P}^T\ \mathbf{u}$ and at the same time cannot increase (usually decreases) the volume $\mathbf{L}^T\ (\mathbf{T} + \mathbf{C})/\sigma_0$.

After the final iteration, a proper subset of active bars of the fully connected ground structure is obtained, delivering the optimal layout. Moreover, at this stage all possible connections are considered, thus the vector $\mathbf{u}$ of nodal displacements must satisfy all constraints $(10)_3$ even for bars not present in the current ground structure, which means that the solution cannot be further improved and is simply the optimal one. For more details on the adaptive version of the ground structure method the reader is referred to Sokół [9, 10].

4. Optimal structures within the L-shaped domain

4.1. The problem setting

Michell structures solving the problems of Fig. 1 will be approximated by the trusses with a very large number of members, using the ground structure method. The analytical solutions are available only for some selected values of the angle α, as explained below. The problem is externally statically determinate, i.e., the reactions are determined by three global equilibrium equations. The problem is equivalent to the three-forces problem, modulo the position of the structure within the plane. Consequently, the theoretical formulation (1), (2), concerning the case of the load being self-equilibrated, applies here.

We apply the ground structure method in the version outlined in Sec. 3. The grid cell dimension b equals $a/64$, which determines the grid $X \subset \overline{\Omega}$

composed of $n = 12545$ nodes. The universe of segments connecting all the distinct pairs of those nodes counts $n(n-1)/2 = 78\,682\,240$ elements. Naturally, due to the non-convexity of the domain, not all segments contribute to the ground structure from which the optimal design will be constructed. For such a number of bars, selecting the members that actually lie within the domain $\overline{\Omega}$ becomes a numerical challenge by itself. To this aim, the authors used a dedicated code that was already employed in Bołbotowski and Sokół [1] and is suited for arbitrary polygonal domains. The target ground structure ends up consisting of 69 775 286 potential bars lying within the closure of the domain $\overline{\Omega}$.

The optimization problems have been solved for 161 choices of the values of the angle α, i.e., for $\alpha = \frac{i\pi}{160}$, $i = 0, ..., 160$. For both positions of the force, 24 representative optimal layouts are selected for presentation; this fairly big number of results makes it possible to show gradually changing layouts of bars for some ranges of angle α on the one hand, and, to disclose the jumps of layouts for some angles α, on the other. The bars in tension are shown in blue, while the bars in compression are shown in red (Fig. 3).

4.2. The force applied at point E

The layouts of optimal trusses for the force applied at point E for selected values of the angle α are presented in Fig. 3 while the corresponding numerical approximations of the optimal volumes are collected in Table 1. The family of solutions parameterized by the angle α starts with the case of $\alpha = 0$ corresponding to the Michell wheel. If the angle increases, the layout changes immediately since, at the hinge B, a horizontal reaction appears implying the appearance of Chan-like domains with bars tangential to the line BA. Consequently, a vertical rib reaching point B appears as non-prismatic, while the circular rib is prismatic, i.e., of constant cross-section throughout its length; in fact, the spokes are orthogonal to the rib. For $\alpha > 0.28\pi$, this non-prismatic rib shortens and a new bar appears linking the hinge B with Chan's subdomain of the structure. For $\alpha \cong 0.352\pi$, the vertical bar CD disappears. For a bigger angle, a new substructure appears and the rib linking B and D becomes a bar of a concentrated cross-section within the structure. For bigger angles the substructure below the line DE reduces until it abruptly disappears when the force is horizontal. For a bigger angle the topology changes; a new bar appears linking point E with the structure's fan domain. Along with the increase of the angle, an empty domain within the optimal structure appears and increases. If the angle reaches 0.89π, a fan domain below the line BC disappears and the layout tends towards the one we have for the angle $\alpha = 0$, but now the tension fibers become compression fibers and vice versa.

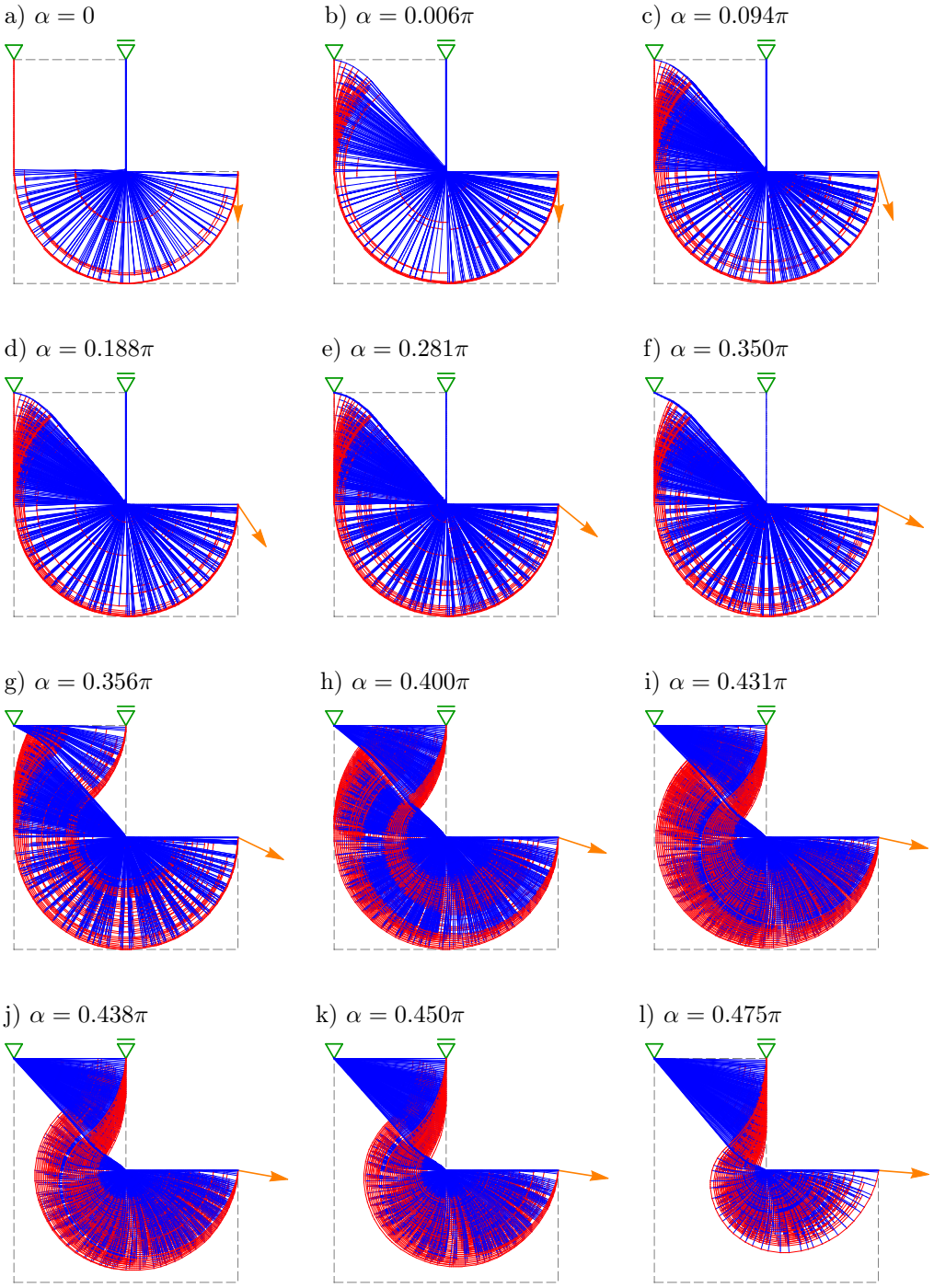

FIG. 3. Truss solutions to Michell problem for the force P applied at point E and for the subsequent, selected values of angle α: from $\alpha = 0$ to $\alpha = \pi$.

m) $\alpha = 0.494\pi$ n) $\alpha = 0.500\pi$ o) $\alpha = 0.550\pi$

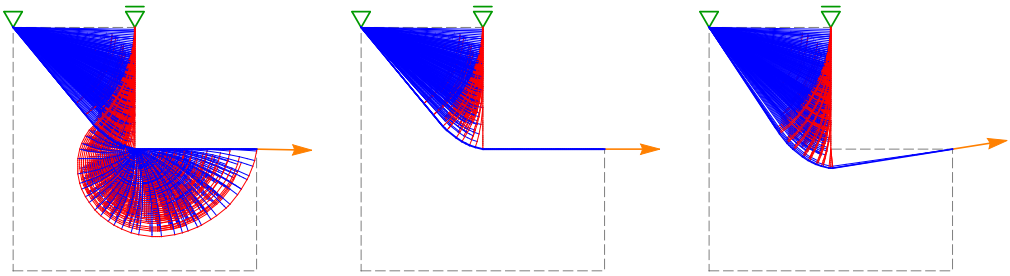

p) $\alpha = 0.594\pi$ q) $\alpha = 0.638\pi$ r) $\alpha = 0.706\pi$

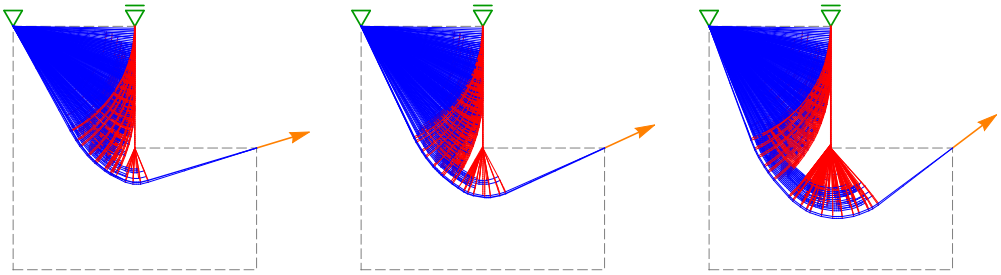

s) $\alpha = 0.756\pi$ t) $\alpha = 0.825\pi$ u) $\alpha = 0.888\pi$

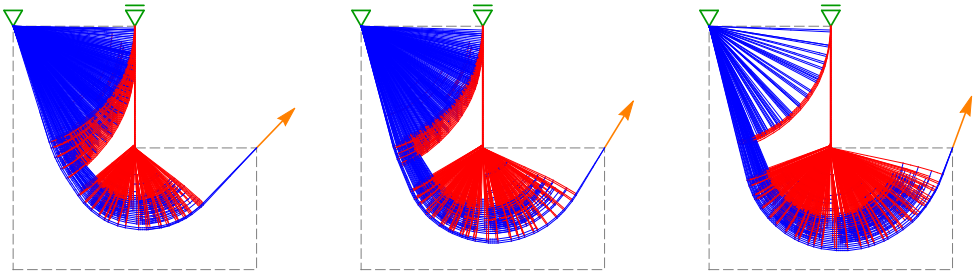

v) $\alpha = 0.894\pi$ w) $\alpha = 0.969\pi$ x) $\alpha = \pi$

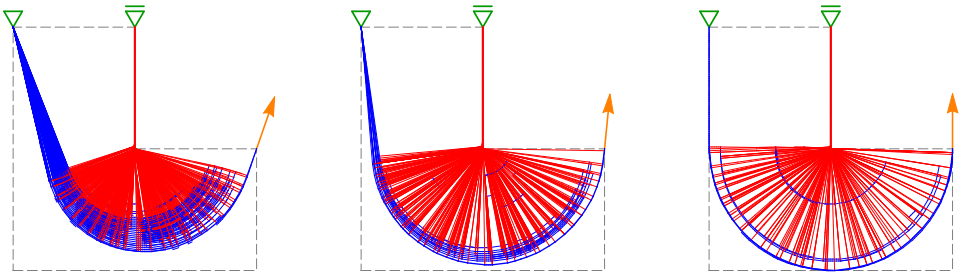

FIG. 3. [Cont.].

TABLE 1. Values of dimensionless volumes V/V_0, $V_0 = Pa/\sigma_0$ of layouts presented in Fig. 3.

Fig.	α	V/V_0	Fig.	α	V/V_0	Fig.	α	V/V_0
3a	$0/160\,\pi$	9.29919	3i	$69/160\,\pi$	4.77943	3q	$102/160\,\pi$	6.00027
3b	$1/160\,\pi$	9.33383	3j	$71/160\,\pi$	4.60975	3r	$113/160\,\pi$	7.05929
3c	$15/160\,\pi$	9.44023	3k	$72/160\,\pi$	4.52500	3s	$121/160\,\pi$	7.75479
3d	$30/160\,\pi$	8.76975	3l	$76/160\,\pi$	4.19595	3t	$132/160\,\pi$	8.53301
3e	$45/160\,\pi$	7.34409	3m	$79/160\,\pi$	3.95505	3u	$142/160\,\pi$	9.00616
3f	$56/160\,\pi$	5.89619	3n	$80/160\,\pi$	3.87251	3v	$143/160\,\pi$	9.03859
3g	$57/160\,\pi$	5.79028	3o	$88/160\,\pi$	4.61524	3w	$155/160\,\pi$	9.27917
3h	$64/160\,\pi$	5.20480	3p	$95/160\,\pi$	5.30179	3x	$160/160\,\pi$	9.29919

The optimal volume is minimal for $\alpha = \pi/2$, see Fig. 4, where $V/V_0 = 3.873$ and $V_0 = Pa/\sigma_0$. At this point, the topology jumps. The volume is maximal for $\alpha \approx 0.0625\pi$, where $V/V_0 = 9.484$. Around the point at $\alpha = 0.352\pi$ the plot of the volume loses its smoothness, which corresponds to the change of topology, as it is visible in Figs 3f and 3g. Note that the layouts and volumes for $\alpha = \pi$ and $\alpha = 0$ are equal due to $\sigma_C = \sigma_T$ (see Figs 3a, 3x and the first and the last row of Table 1).

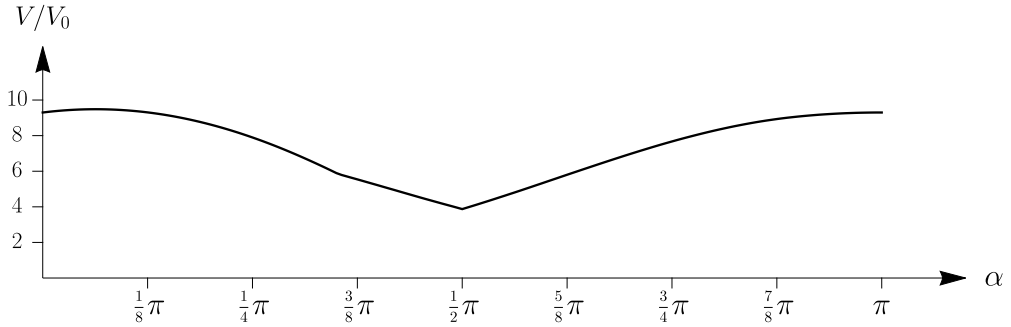

FIG. 4. Variation of the volume V/V_0, $V_0 = Pa/\sigma_0$ for the force P applied at point E and for subsequent values of the angle α.

4.3. The force applied at point F

The layouts of optimal trusses for the force applied at point F for selected values of α are presented in Fig. 5. The corresponding numerical approximations of the optimal volumes are collected in Table 2. The family of solutions starts from the layout for $\alpha = 0$, solved analytically in Lewiński *et al.* [6, 7]. When α increases the layout changes abruptly, since a horizontal reaction at node B appears (see Fig. 5b). For a bigger α, see Figs 5d–f, a sort of a ligament (i.e., a linking bar) radiating from B appears and its length increases. When α becomes

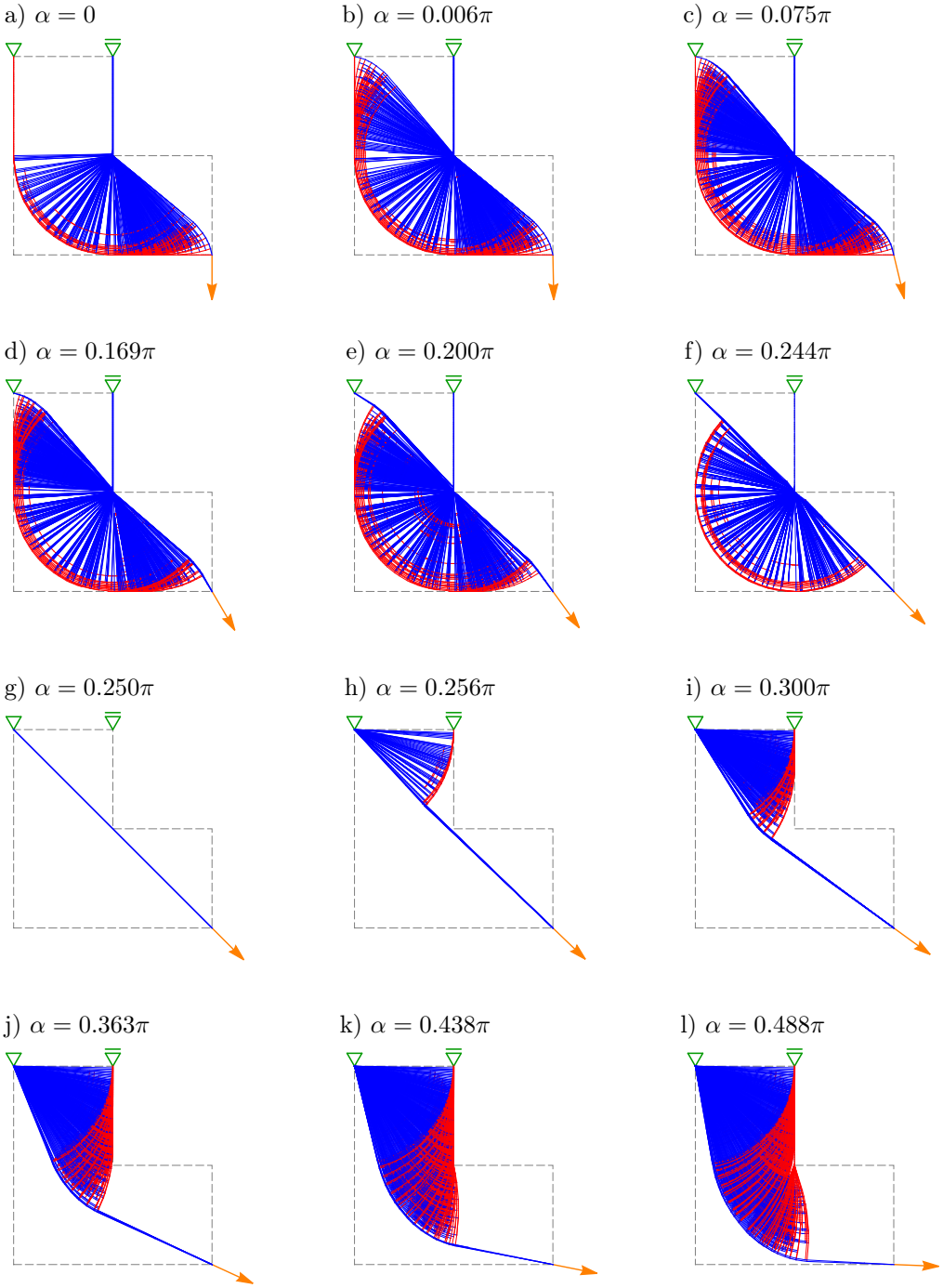

FIG. 5. Truss solutions to Michell problem for the force P applied at point F and for the subsequent values of angle α: from $\alpha = 0$ to $\alpha = \pi$.

m) $\alpha = 0.500\pi$

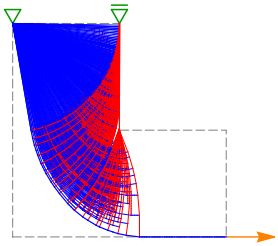

n) $\alpha = 0.506\pi$

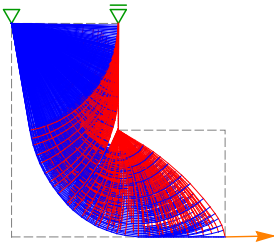

o) $\alpha = 0.563\pi$

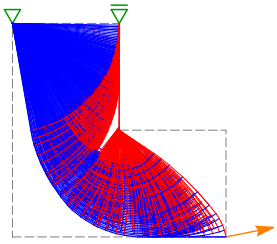

p) $\alpha = 0.625\pi$

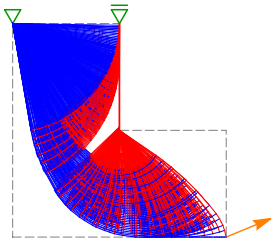

q) $\alpha = 0.688\pi$

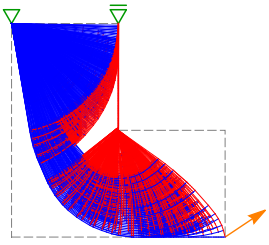

r) $\alpha = 0.750\pi$

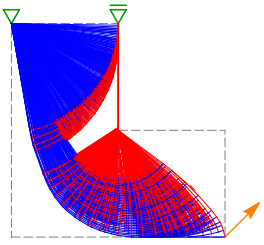

s) $\alpha = 0.819\pi$

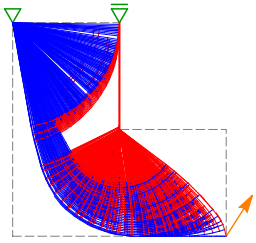

t) $\alpha = 0.881\pi$

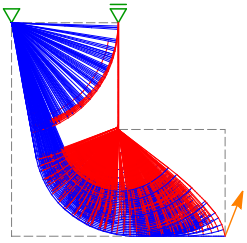

u) $\alpha = 0.888\pi$

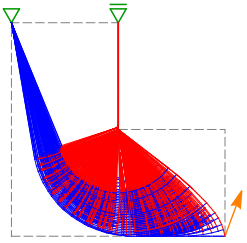

v) $\alpha = 0.963\pi$

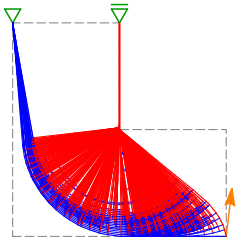

w) $\alpha = 0.994\pi$

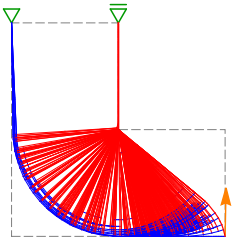

x) $\alpha = \pi$

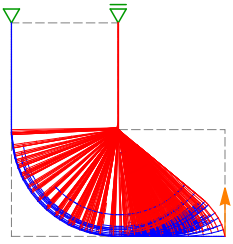

Fig. 5. [Cont.].

TABLE 2. Values of dimensionless volumes V/V_0, $V_0 = Pa/\sigma_0$ of layouts presented in Fig. 5.

Fig.	α	V/V_0	Fig.	α	V/V_0	Fig.	α	V/V_0
5a	$0/160\,\pi$	9.02210	5i	$48/160\,\pi$	3.70956	5q	$110/160\,\pi$	11.91853
5b	$1/160\,\pi$	8.91657	5j	$58/160\,\pi$	5.13057	5r	$120/160\,\pi$	12.19217
5c	$12/160\,\pi$	7.53975	5k	$70/160\,\pi$	7.01201	5s	$131/160\,\pi$	11.96541
5d	$27/160\,\pi$	5.13008	5l	$78/160\,\pi$	8.24917	5t	$141/160\,\pi$	11.28728
5e	$32/160\,\pi$	4.24253	5m	$80/160\,\pi$	8.54700	5u	$142/160\,\pi$	11.19634
5f	$39/160\,\pi$	2.99914	5n	$81/160\,\pi$	8.71310	5v	$154/160\,\pi$	9.83852
5g	$40/160\,\pi$	2.82843	5o	$90/160\,\pi$	10.05749	5w	$159/160\,\pi$	9.16257
5h	$41/160\,\pi$	2.91961	5p	$100/160\,\pi$	11.19798	5x	$160/160\,\pi$	9.02210

equal to $\pi/4$ the whole structure reduces to a single bar connecting node B of the support with F, where the force is applied. Just for this angle, the volume is the smallest, see Fig. 6. For α bigger than $\pi/4$ the layout changes essentially, with a characteristic ligament connecting point F with the body of the structure, see Figs 5h–j. From then we see how the re-entrant corner D affects the optimal layout. We note that a specific fan of origin at D of curvilinear fibers is formed. On the other hand, an empty sub-region adjacent to the line CD arises and grows with increasing α. This region will disappear at $\alpha \approx 0.888\pi$. Starting with $\alpha = \pi/2$, a new Chan's region is growing, adjacent to the line AF. This region will be present up to the last value $\alpha = \pi$. The layout jumps between (t) and (u), Fig. 5: the circular fan of origin at B ceases to be necessary for $\alpha > 0.88\pi$. The final layout (x) is the same as the first one (a), only the bars that were in tension are now in compression and vice versa (see Figs 5a, 5x and the first and the last row of Table 2).

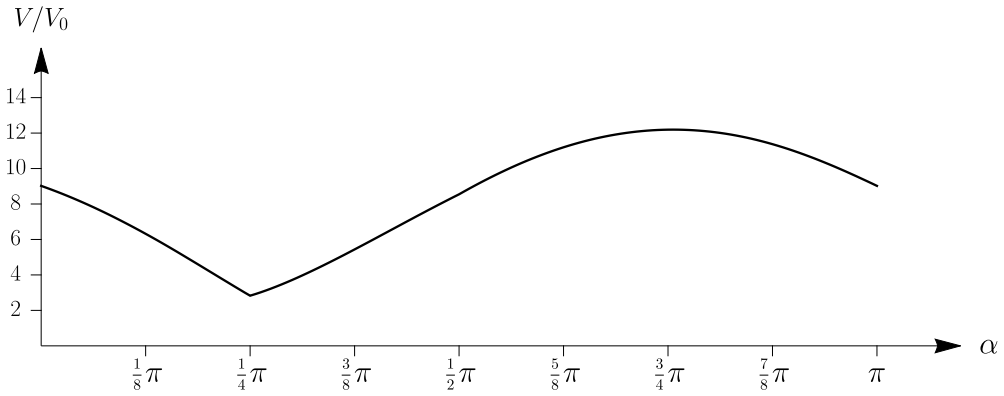

FIG. 6. Variation of the volume V/V_0, $V_0 = Pa/\sigma_0$ for the force P applied at point F and for subsequent values of the angle α.

The plot of volume V decreases between $\alpha = 0$ and $\alpha = \pi/4$, attaining minimum at $\alpha = \pi/4$, where the plot ceases to be smooth. Then the plot of V increases up to the maximal value $V = 12.194V_0$ for $\alpha \approx 0.756\pi$ and decreases to the initial value (for $\alpha = 0$) because $\sigma_C = \sigma_T$.

Some of the numerical layouts presented in Figs 3 and 5 have the analytical counterparts, discussed in detail by Lewiński *et al.* [7] and Sec. 4.14 of the book by Lewiński *et al.* [8]. The numerically found layouts for which the analytically constructed layouts are available are set up in Table 3. The volume of the optimal structures (with the multiplication factor σ_0) is calculated as the virtual work of the applied force and the reactions, the virtual displacement field being expressed by Eqs (11)–(19) in Lewiński *et al.* [7]. In the case of the force applied at point E and $\alpha \leq \pi/4$, the exact volume of the optimal structure is given by

$$V = \frac{Pa}{\sigma_0}\left[(3 + 2\pi)\cos\alpha + \xi \sin\alpha\right] \tag{12}$$

(the derivation is omitted here), where ξ is defined as

$$\xi = G_0(\alpha_0, \alpha_0) + 2F_2(\alpha_0, \alpha_0) - 1, \tag{13}$$

α_0 is the root of the transcendental equation

$$F_1(\alpha_0, \alpha_0) - F_3(\alpha_0, \alpha_0) = 1 \tag{14}$$

and the special functions $G_n(\cdot, \cdot)$, $F_n(\cdot, \cdot)$ are defined in Sec. 4.2.3 of Lewiński *et al.* [8]. The solution of (14) is $\alpha_0 \approx 0.87806028$ (alternatively 50.309148°), hence $\xi \approx 1.8659188$.

The comparison of analytical and numerical solutions for selected layouts of Figs 3 and 5 are shown in Table 3. The relative errors of numerical solutions with respect to analytical ones are smaller than 0.2%, which clearly indicates the efficiency of the applied numerical method.

TABLE 3. Comparison of numerical V_n/V_0 and analytical V_a/V_0 volumes, $V_0 = Pa/\sigma_0$.

Figure	α	V_a/V_0	V_n/V_0	Relative error [%]
3a and 3x	0	9.283185	9.28755	0.047
3b	1/160 π	9.318031	9.33383	0.170
3c	15/160 π	9.425102	9.44023	0.161
3d	30/160 π	8.755335	8.76975	0.165
5a and 5x	0	9.007675	9.01246	0.053
5g	40/160 π	2.828427	2.82843	0.000

5. Final remarks

This paper discussed a numerically efficient discrete approach to Michell problem posed for the L-shaped design domain. The link between the continuous setting of the Michell problem (1), (2) and the discrete truss optimization via the ground structure method was established through the two-point condition (6). The ground structure method was employed for the non-convex L-shaped domain for two positions of the point load and sequence of its directions α ranging from 0 to π. Selected numerical results compare favorably with the available exact analytical solutions.

This paper has dealt exclusively, theoretically and numerically, with the case of equal permissible stresses in tension and compression: $\sigma_T = \sigma_C$. Although the general case of $\sigma_T \neq \sigma_C$ has not been tackled, the solutions to the problem discussed turned out to be easily obtainable. Indeed, the problems studied can be treated as special cases of the three forces problem, here referring to the L-shaped domain. As mentioned, the structures considered here are simply supported. Thus, the reaction forces at supports (points B and C in Fig. 1) are uniquely defined and can be treated as external loads of the same magnitudes. This type of problem with the self-equilibrated system of external forces was thoroughly studied by Maxwell, see Lewiński *et al.* [8], Sec. 2.2.3. Maxwell discovered that all trusses transmitting the given system of loads are characterized by an invariant $\mathcal{M}$ (see (16) below), called Maxwell number, and then Michell proved that for this class of problems the optimal layout is independent of the ratio σ_T/σ_C. To obtain the final solution for $\sigma_T \neq \sigma_C$, it is sufficient to solve the problem for $\sigma_T = \sigma_C = \sigma_0$ and then properly scale the cross-section areas by σ_0/σ_T and σ_0/σ_C for bars in tension and compression, respectively. The volume of such a new truss is equal to

$$V_{TC} = \frac{1}{2}\left(\frac{1}{\sigma_T} + \frac{1}{\sigma_C}\right)(V\sigma_0) + \frac{1}{2}\left(\frac{1}{\sigma_T} - \frac{1}{\sigma_C}\right)\mathcal{M}, \tag{15}$$

where V is the volume of the optimal truss for permissible stresses in tension and compression being equal to σ_0, see Eq. (2.70) in Lewiński *et al.* [8]. The quantity $\mathcal{M}$ is defined as

$$\mathcal{M} = \sum_i \mathbf{P}_i \cdot \mathbf{r}_i, \tag{16}$$

where $\mathbf{P}_i$ represent the external forces applied (here – all forces including the reactions at B and C) and $\mathbf{r}_i$ are radii linking an arbitrary pole with the points of application of the given forces.

As an example, we consider the force applied at point E with the angle $\alpha = 0.825\pi$, see Fig. 7. We choose the pole as point B, then the Maxwell number

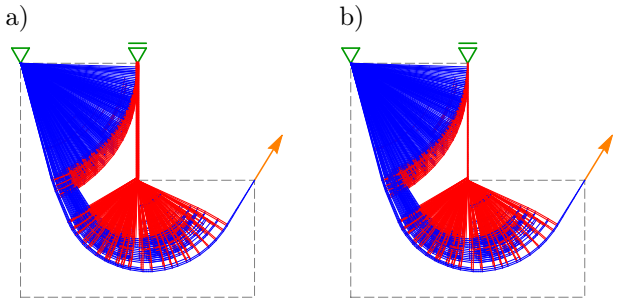

FIG. 7. Truss solutions to Michell problem for the force P applied at point E and for angle $\alpha = 0.825\pi$ for the case: a) $\sigma_T = \sigma_C = \sigma_0$, the optimal volume reads $V = 8.53Pa/\sigma_0$, b) $\sigma_T = \sigma_0$, $\sigma_C = 2\sigma_0$, the optimal volume reads $V_{TC} = 6.45Pa/\sigma_0$.

is expressed by $\mathcal{M} = P\,[\sin\alpha, \cos\alpha] \cdot [2a, a]$ and equals $0.1923Pa$. Let us assume $\sigma_T = \sigma_0, \sigma_C = 2\sigma_0$ and compute the volume according to (15). The result is $V_{TC} = 6.45Pa/\sigma_0$ and has been confirmed by the ground structure method, see Fig. 7b.

Acknowledgements

This paper was prepared within the Research Grant no 2019/33/B/ST8/00325 financed by the National Science Centre (Poland), entitled: *Merging the optimum design problems of structural topology and the optimal choice of material characteristics. The theoretical foundations and numerical methods.*

The first author would also like to thank the National Science Centre (Poland) for financing the Research Grant no 2015/19/N/ST8/00474 entitled: *Topology optimization of thin elastic shells – a method synthesizing shape and free material design.*

References

1. K. Bołbotowski, T. Sokół, New method of generating Strut and Tie models using truss topology optimization, [in:] M. Kleiber, T. Burczyński, K. Wilde, J. Górski, K. Winkelmann, Ł. Smakosz [Eds], *Advances in mechanics: Theoretical, computational and interdisciplinary Issues*, pp. 97–100, CRC Press, 2016.

2. G. Bouchitté, I. Fragalà, Optimality conditions for mass design problems and applications to thin plates, *Archive for Rational Mechanics and Analysis*, **184**(2): 257–284, 2007.

3. G. Bouchitté, W. Gangbo, P. Seppecher, Michell trusses and lines of principal action, *Mathematical Models and Methods in Applied Sciences*, **18**(9): 1571–1603, 2008.

4. M. Gilbert, A. Tyas, Layout optimization of large-scale pinjointed frames, *Engineering Computations*, **20**(8): 1044–1064, 2003.

5. W.S. Hemp, *Optimum structures*, Oxford, Clarendon Press, 1973.

6. T. Lewiński, G.I.N. Rozvany, Exact analytical solutions for some popular benchmark problems in topology optimization III: L-shaped domains, *Structural and Multidisciplinary Optimization*, **35**(2): 165–174, 2008, doi: 10.1007/s00158-007-0157-8.

7. T. Lewiński, G.I.N. Rozvany, T. Sokół, K. Bołbotowski, Exact analytical solutions for some popular benchmark problems in topology optimization III: L-shaped domains revisited, *Structural and Multidisciplinary Optimization*, **47**(6): 937–942, 2013, doi: 10.1007/s00158-012-0865-6.

8. T. Lewiński, T. Sokół, C. Graczykowski, *Michell structures*, Springer International Publishing AG, Cham, Switzerland, 2019, doi: 10.1007/978-3-319-95180-5.

9. T. Sokół, Multi-load truss topology optimization using the adaptive ground structure approach, [in:] T. Łodygowski, J. Rakowski, P. Litewka [Eds], *Recent advances in computational mechanics*, pp. 9–16, CRC Press, London, 2014.

10. T. Sokół, A new adaptive ground structure method for multi-load spatial Michell structures, [in:] M. Kleiber, T. Burczyński, K. Wilde, J. Górski, K. Winkelmann, Ł. Smakosz [Eds], *Advances in mechanics: Theoretical, computational and interdisciplinary issues*, pp. 525–528, CRC Press, 2016.

11. G. Strang, R.V. Kohn, Hencky-Prandtl nets and constrained Michell trusses, *Computer Methods in Applied Mechanics and Engineering*, **36**(2): 207–222, 1983.

Received January 31, 2020; revised version May 19, 2020.